



VICTORIA UNIVERSITY
MELBOURNE AUSTRALIA

Frequency performance analysis of multi-gain droop controlled DFIG in an isolated microgrid using real-time digital simulator

This is the Published version of the following publication

Datta, Ujjwal, Kalam, Akhtar and Shi, Juan (2019) Frequency performance analysis of multi-gain droop controlled DFIG in an isolated microgrid using real-time digital simulator. *Engineering Science and Technology, an International Journal*. ISSN 2215-0986

The publisher's official version can be found at
<https://www.sciencedirect.com/science/article/pii/S2215098619318014>
Note that access to this version may require subscription.

Downloaded from VU Research Repository <https://vuir.vu.edu.au/40972/>

HOSTED BY



ELSEVIER

Contents lists available at ScienceDirect

Engineering Science and Technology, an International Journal

journal homepage: www.elsevier.com/locate/jestch

Full Length Article

Frequency performance analysis of multi-gain droop controlled DFIG in an isolated microgrid using real-time digital simulator

Ujjwal Datta*, Akhtar Kalam, Juan Shi

College of Engineering and Science, Victoria University, P.O. Box 14428, Victoria 8001, Melbourne, Australia

ARTICLE INFO

Article history:

Received 16 August 2019

Revised 30 September 2019

Accepted 28 November 2019

Available online xxxxx

Keywords:

Dynamic multi-gain droop

Primary frequency control

Wind energy

Pitch control

ABSTRACT

With the increased share of wind power in Microgrid (MG), wind farm is expected to have significant contribution in overall grid frequency regulation. Wind farm impersonating synchronous generator with conventional droop control method may threaten the grid stability during low frequency oscillations. In this paper, synthetic inertia with a novel frequency dependent multi-gain droop control strategy is proposed to regulate wind farm for providing primary frequency response. The proposed multi-gain droop control is combined with a proportional and proportional-integral type pitch angle controller for comparative analysis. A 20% power reserve is conserved for primary frequency regulation. The influence of multi-gain parameters (power-frequency) and numerous power margin of wind farm is also examined under different contingency events. The relative performances of the proposed control scheme are investigated in a small isolated MG with 20.8% and 41% wind penetration in real-time. Simulation results show that it is possible to achieve optimum frequency control performance with the proposed multi-gain droop control scheme compared with the conventional droop control. It is also found that parameter selection for multi-gain droop control portrays significant domination on the overall frequency control outcome. Moreover, the proposed multi-gain droop method performs satisfactorily at different power margin of wind farm.

© 2019 Karabuk University. Publishing services by Elsevier B.V. This is an open access article under the CC BY-NC-ND license (<http://creativecommons.org/licenses/by-nc-nd/4.0/>).

1. Introduction

Wind energy is one of the dominant renewable energy sources (RES) in the present electricity supply industry and is expected to have a similar rising tendency in the future. This trend has become possible due to the rapid transition of commercialized wind technology, continued cutback in both onshore and offshore wind costs and government legislations [1]. A doubly fed induction generator (DFIG) is at the forefront of the available wind technologies due to their ability to produce maximum power at changing wind speeds and regulate active and reactive power output [2,3].

New technical challenges emerge with the increased share of wind energy penetration that threatens the security and reliability of power system. The main concern arises owing to the intermittent behavior of the wind energy and its negative impact on overall grid performance. The base-load unit is heavily stressed while balancing rapid change in alternating wind power and this largely affects the life cycle of the base-load unit and increases operation and maintenance costs. In addition, present-day power electronics

based variable speed wind turbines do not contribute to system inertia inherently and therefore affect adversely on grid frequency control. Conventionally, synchronous generators take the responsibility to mitigate frequency imbalances in a grid-connected power system. However, in an isolated Microgrid (MG), such facilities are not available. Energy storage (ES) such as a battery [4], flywheel [5] or capacitor [6] is one of the alternatives to provide frequency regulation services in an isolated power system. Nevertheless, ES is an expensive selection for an isolated MG. Hence, it is crucial that wind farm participates in frequency regulation that can eventually contribute to the technical and economic benefit of the MG with the increased penetration of wind energy.

Generally, DFIG is operated in maximum power point tracking (MPPT) mode [7] to maximize the power output at a given wind speed. In order to participate in frequency regulation, wind turbines take part in energy exchange by forcing their power operating point deviated from the MPPT point to a different level. This may reduce the overall amount of wind energy contribution to the grid depending on the total energy exchange during the primary frequency response (PFR) service. This is referred to as deloading. Many research works have proposed emulating the behavior of conventional synchronous machines by wind turbines

* Corresponding author.

E-mail address: ujjwal.datta@live.vu.edu.au (U. Datta).

to deal with the technical challenges of reduced inertia and minimize the issues of wind energy application in the existing grid. In [8–10], the wind turbine is used to emulate inertia (IE) is demonstrated to provide more reliable results in reducing the rate-of-change-of-frequency (ROCOF), achieving improved damping performance and thus avoiding the adverse impact of increased wind energy. A power referenced inertial control scheme for a wind turbine is proposed in [11] to participate in frequency regulation that demonstrated a promising outcome. A similar control strategy of IE is presented in [12] that shows smoother and enhanced frequency response under various disturbed conditions. In [13], the authors have demonstrated that with the increased level of wind penetration and IE of a wind turbine, the overall stability performance of the grid becomes very poor and this can limit wind energy penetration considering reliability issues related to the wind energy. The droop control in [14,15] revealed that it is possible to minimize frequency deviations and achieve improved frequency regulation which is technically more sophisticated than the previous method. Considering such technical challenges of wind turbine in frequency regulation, researchers have proposed a coordinated control to achieve better frequency regulation of wind active power in response to frequency variation [16–18]. The aim is to exploit the stored kinetic energy of wind turbine, providing flexible frequency control by the wind turbine without the loss of security of wind turbines and the grid. The case studies demonstrate that the technical challenges of wind turbine penetration such as higher frequency excursion and slower frequency recovery with lower steady-state frequency can be minimized [19–21]. Hence, the results indicate that this can ensure better frequency regulation, provide enhanced stability performance of the system and can potentially support large wind energy application in the grid without compromising the security of the system. A quadratic droop gain is proposed in [22] and compared with conventional linear droop gain. However, IE is not incorporated in the design and also the improvement in system frequency is very insignificant between the conventional and proposed method.

Many research works have presented droop and IE combined methods that aim to temporarily increase or decrease the power output of wind turbine and participate in frequency regulation [23–25]. Coordinated control of IE and droop is presented in [26,27] to improve the frequency characteristics of the grid. Another combined virtual inertia control proposed in [28] showed that operating point and pitch angle control have a noticeable impact on the inertial performance of wind turbine. The authors in [29] presented a frequency regulated pricing scheme for improving the frequency profile. A time-dependent inertial and droop control gain is proposed in [30] which operates based on the expected response time of frequency. However, with varying network conditions, this method may not perform satisfactorily.

When the wind speed is of the rated speed up to the cut-out speed, pitch angle control limits the over-speeding of wind turbines to avoid mechanical damage of the wind turbine in order to produce the rated power output. This in turn diminishes power oscillations and hence scales down stress in the network [31]. In order to deal with the threats caused by variable wind speed on frequency stability, the coordinated inertia, droop and pitch control plays an essential role. It is observed that an improved stability performance of the wind turbine and frequency security can be ensured with the coordinated control during frequency transients [32–34].

All the aforementioned works of wind turbine in PFR are focused on fixed droop gain values or time dependent dynamic gains. However, as the measurement of deloaded power is not

constant with the changing wind speed conditions, adopting a classical linear gain may lead to higher oscillations in DFIG power output [35] and may affect the performance of frequency stability. These concerns have led researchers to investigate and adopt non-linear, dynamic droop gain that can assure better frequency regulation of wind turbine during transient periods. In [36], a dynamic droop gain is proposed for frequency control that prevents the over-deceleration of DFIG during transient periods and ensures better operational stability. On the other hand, the study in [37] shows that the proposed efficiency droop improves the steady-state and transient frequency performance of a MG. However, the maximum improvements in frequency response are the same regardless of the adopted droop methods. Varying droop gain is proposed in [38] to secure optimal frequency regulation during a disturbance occurrence period and thus minimizing the strain of wind energy penetration. However, the adjustment of droop gain is not autonomous and thus required to be adjusted manually with the changes in wind speed. In [39], to reduce the energy losses of wind turbine, a variable gain is proposed while participating in frequency regulation. Nevertheless, the study is limited to over-frequency supports only. A time variable droop scheme is proposed in [40] to prevent large frequency oscillations during the variations in wind speed, nonetheless, this may not be effective with the changing operating conditions due to inadequate recovery time settings and may result in large frequency excursions which can lead to frequency instability.

The earlier studies came with several shortcomings such as some studies have either considered fixed gain or wind speed dependent variable gain and also maximum improvements in overall frequency stability performance are limited. In this paper, the potential of DFIG for providing PFR is proposed and a novel dynamic multi-gain droop control mechanism is presented to enhance MG frequency stability and ensure robust regulation of DFIG during frequency transients. This method is based on the study presented in [41] for electric vehicle charge control. The method is incorporated in DFIG controller of wind turbine with other control schemes to generate the reference signal for the rotor side converter of DFIG. The method has not been applied in regulating DFIG for PFR in earlier or current studies. The main contributions of this study are as follows:

- A frequency dependent dynamic multi-gain droop control mechanism is proposed for an aggregated wind farm providing PFR in an isolated MG. This control approach principally depends on the depth of frequency deviation i.e. high and low sensitive regions. The low-frequency variation is remarked as a highly sensitive region having lower power contribution in PFR for the dedicated frequency deviation territory and high power contribution for low sensitive regions. An emulated inertia control loop is further added with the proposed multi-gain droop control to provide better frequency regulation.
- The robust performance of the proposed control scheme is investigated in combination with two different types of pitch angle controllers, proportional (P) and Proportional-Integral (PI), once at a time.
- In addition, this paper thoroughly investigates the domination of selecting different multi-gain droop parameters (power vs frequency) on achieving enhanced frequency control outcome.
- The different levels of power margin i.e. the intensity of wind farm participation in primary frequency control is also explored to further demonstrate the efficacy of the proposed multi-gain droop control scheme compared to conventional droop control method.

- Furthermore, an increased level of wind penetration is also simulated to demonstrate the efficacy of the proposed multi-gain droop control approach.
- Compared to earlier studies in [23–30], this study is carried out in real-time digital simulator (RTDS) which is competent to emulate physical entity and thus brings a strong value in performance analysis of the proposed control approach.

The rest of the paper is outlined as follows. A brief discussion on wind turbine, MG modeling and pitch angle controls are presented in Section 2. Section 3 discusses the conventional droop and inertial control schemes for providing primary frequency response. Detailed discussion on the proposed multi-gain droop control scheme is illustrated in Section 4. The performance of the proposed controller is demonstrated through Matlab/Simulink simulation and discussed in Section 5. An overall conclusion of the paper is drawn in Section 6.

2. Conventional fixed gain droop control and inertial control schemes

Conventionally, synchronous generators mitigate any temporary imbalances of generated and demanded power by providing an instant inertial response (IR) from the stored kinetic energy. Similar inertial control loop can be incorporated with the MPPT controller of DFIG to mimic the behavior of conventional generators in the case of power imbalances. For the inertial response, the DFIG can temporarily overproduce power during which it will slow down and inject power into the grid and vice versa. The conventional droop with inertia is shown in Fig. 1. The IR followed by a disturbance can be defined as in (1):

$$\Delta P_{IR} = K_{IR} \frac{d}{dt} \Delta f = 2H_w \frac{d}{dt} \Delta f \quad (1)$$

where, H_w is the inertial gain of wind turbines, Δf is the measured frequency deviation of the actual grid and the reference frequency. The power of wind turbine is temporarily adjusted to obtain IR. The wind turbine responds to under-frequency by slowing down the turbine and extracting stored kinetic energy. According to (1), the rise/fall of IR is calculated with an associated change in frequency. A small deadband of ± 0.05 Hz is included to avoid IR response for a very small change in frequency and the inertial gain is selected as 0.2 pu. The IR is more dominant at the initial stage of frequency deviation followed by a disturbance. ROCOF loop is less effective once the primary frequency control takes over. hence, with the growing frequency deviation, droop loop plays crucial role in an overall contribution of primary frequency regulation. However, wind turbine needs to be operated below MPPT to extract sufficient

power margin for primary frequency regulation. Thus, deloading takes place by shifting the operating point of wind turbine to the left or right of MPPT by under/over-speeding and creating temporary power reserve to mitigate grid frequency variation.

The conventional droop can be written as in (2):

$$\Delta P_{PFR} = \frac{1}{R} \Delta f \quad (2)$$

where, $\frac{1}{R}$ is the droop gain. The power reference of PFR and IR are added with the reference power of wind turbine at MPPT (P_{w0}) to generate updated power reference (P_{wind}^{ref}) as shown in Fig. 1 and in (3). The values of ΔP_{PFR} and ΔP_{IR} are negative for a positive frequency change to reduce power output and positive for a negative frequency change to increase power output at DFIG output terminal and vice versa. The "1/R" value is selected as 25 that defines for a change of 4% in frequency, the power will change by 100%. The maximum amount of power reserve is 20% which is activated for the maximum frequency change of 0.008 pu beyond the deadband of 0.002 pu [42]. Since the droop gain is a multiple of frequency deviation, ΔP_{PFR} will increase with the increase of Δf . Therefore a deloading limit denoted as D_{lim} in Fig. 1 is enclosed and min/max value is selected as 0.2 pu to restrict 20% power margin of wind farm.

$$P_{wind}^{ref} = P_{w0} - \Delta P_{PFR} - \Delta P_{IR} \quad (3)$$

Since the gains of both controllers are fixed, a large gain may result in rapid acceleration/deceleration, especially during the droop control at low frequency oscillations as it has major contribution in PFR.

3. The proposed multi-gain droop control strategy

According to (2), a small value of R may ensure wind farm participation at a higher rate in frequency regulation. But, adopting such a low value may react abnormally for smaller oscillations mainly near the edges of standard non-operating frequency band (NOFB). Therefore, a variable droop gain is imperative to address such stability concern with wind farm participating in PFR.

In the presented study, the proposed multi-gain droop control regulates the sensitivity of the wind farm's participation when DFIG takes part in frequency regulation. This enables the adjustment of gain depending on the various circumstances of frequency change. The proposed multi-gain droop control mechanism is demonstrated in Fig. 2 which replaces the fixed droop gain control in Fig. 1. The multi-gain droop is combined with inertia control loop as shown in Fig. 1. It is worth noting that the gains are calculated for a deviation in frequency (Δf), not the actual frequency.

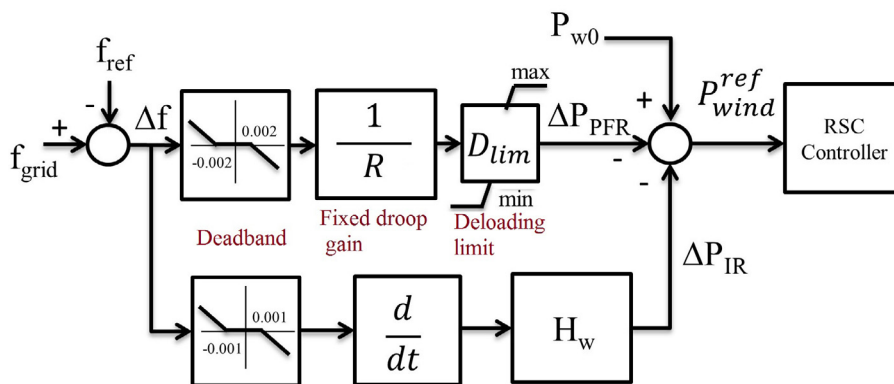


Fig. 1. Inertial and Conventional Fixed Droop Gain Control.

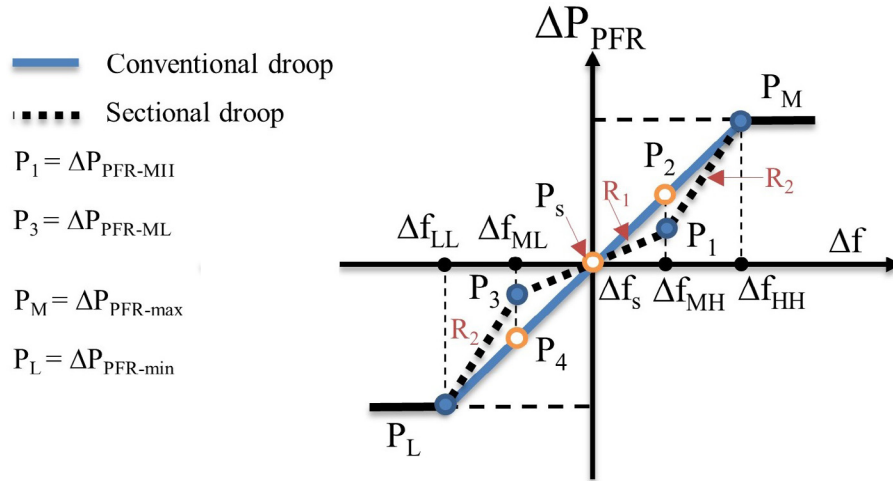


Fig. 2. The Proposed Multi-gain Droop Control Strategy.

Hence, when frequency value stays within the defined deadband regions, the change in frequency $\Delta f = 0$. The multi-gain droop activates when the frequency deviates by 100 mHz from the nominal value as in conventional droop. Therefore, wind farm does not participate within that NOFB i.e. $P_s = 0$. The multi-gain droop design is achieved by selecting separate droop gains for two various frequency operating regions. As indicated in the figure, the wind farm response is segregated in high and low sensitive region.

In order to implement the proposed multi-gain control, the linear droop is split into two clusters depending on the range of frequency deviation. Each cluster is designed to regulate its power output according to the calculated frequency deviation such as reduce a considerable number of active power participation during a smaller frequency variation. This ensures a limited share of wind farm for minor changes and greater percentage for higher order deviations of system frequency. As shown in Fig. 2, the lower frequency deviation (between Δf_{ML} (medium-low) and Δf_{MH} (medium-high)) is remarked as highly sensitive region since the frequency deviation is small in this region. Hence, linear relationship with power-frequency (P-f) characteristics in this region may lead to large oscillations, in particular with the large-sized wind farm. In addition, with the increased share of wind farm in PFR service may worsen the grid frequency for high droop gain in this region. Therefore, the droop gain is reduced considerably for the highly sensitive region and thus the droop value has shifted ΔP_{PFR} to a new point at P_1 and P_3 from the conventional droop point of P_2 and P_4 . This ensures the regulation of the reduced amount of wind power output for highly sensitive regions. The aim is to ensure stronger and smoother regulation capability of wind farm within the same region of frequency variation compared to the conventional droop based regulation. Following the frequency trend, the intensity of DFIG participation accelerates when the frequency deviation increases above Δf_{MH} and drops below Δf_{ML} . The maximum participation of wind farm is designed to be activated for the designated point of frequency deviation; $\Delta P_{PFR-max}$ for a frequency deviation of Δf_{HH} and $\Delta P_{PFR-min}$ for a value of Δf_{LL} . The combination of median and maximum P-f provides the complete regulation of wind power output with respect to the relevant changes in frequency. This accomplishes multi-gain droop value for corresponding frequency deviation which in turn regulates the power output of DFIG. The maximum power margin of wind farm for the conventional and the proposed multi-gain droop is the same.

The mathematical expression of DFIG power for multi-gain droop can be written as in (4):

$$\Delta P_{PFR} = \begin{cases} P_M & \text{if } \Delta f \geq \Delta f_{HH} \\ P_1 + P_{WT1} & \text{if } \Delta f_{MH} < \Delta f < \Delta f_{HH} \\ P_{WT2} & \text{if } 0 < \Delta f < \Delta f_{MH} \\ 0 & \text{if } \Delta f = 0 \\ P_{WT3} & \text{if } \Delta f_{ML} < \Delta f < 0 \\ -P_3 - P_{WT4} & \text{if } \Delta f_{LL} < \Delta f < \Delta f_{ML} \\ P_L & \text{if } \Delta f \leq \Delta f_{LL} \end{cases} \quad (4)$$

where, the corresponding multi-gain droop coefficients are:

$$\begin{aligned} P_{WT1} &= \frac{P_M - P_1}{\Delta f_{HH} - \Delta f_{MH}} (\Delta f - \Delta f_{MH}) \\ P_{WT2} &= \frac{P_1 - P_s}{\Delta f_{MH}} \Delta f \\ P_{WT3} &= \frac{P_L - P_s}{\Delta f_{ML}} (-\Delta f) \\ P_{WT4} &= \frac{P_L - P_3}{\Delta f_{ML} - \Delta f_{LL}} (-\Delta f + \Delta f_{ML}) \end{aligned} \quad (5)$$

The associated power outputs of DFIG for the relevant frequency deviation can be calculated as in (5). The values of P_{WT2} and P_{WT3} are the DFIG power output for highly sensitive positive and negative regions in regard to lower frequency deviation which varies in accordance with P-f droops. Similarly, the power output references for low sensitive regions are represented by P_{WT1} and P_{WT4} which are added with median power output reference of DFIG, P_1 and P_3 . In the end, the maximum and minimum power output of DFIG are constrained within P_M and P_L , respectively. The droop action initiates with the rise/fall of Δf value. The decreased/increased frequency error Δf will push wind turbine to regulate their power output. The droop gain is reduced near the edges of low-frequency corridor to avoid rapid high power output. The adopted conventional and multi-gain droop parameter settings are shown in Fig. 3. The maximum P-f droop of wind farm is selected as $\Delta P_{PFR} = 0.2$ pu for a frequency deviation of 0.01 pu of the nominal value. As the frequency deadband is 0.002 pu, hence ΔP_{PFR} is calculated for a value of $\Delta f = 0.008$ pu. The intermediate

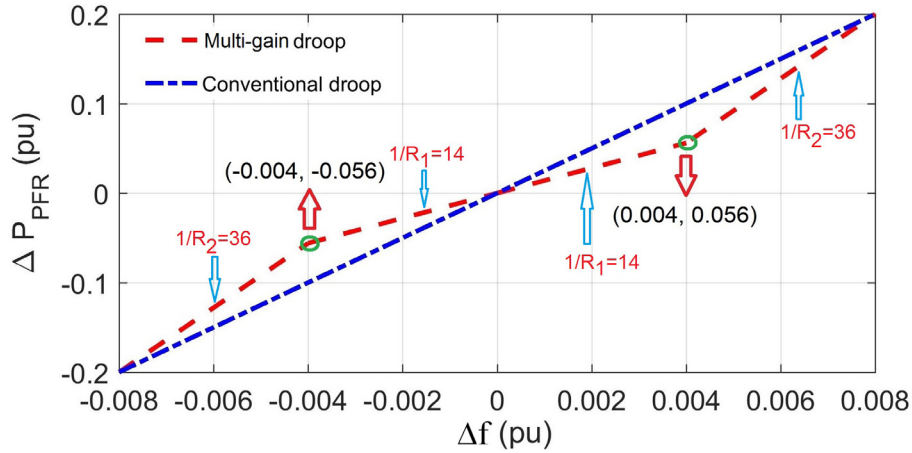


Fig. 3. Conventional and Sectional Droop with the Selected Parameters.

droop operating point is selected as $\Delta f = 0.004$ pu that defines a corresponding value of $\Delta P_{PFR} = 0.056$ pu, the droop gain of $1/R_1 = 14$ and $1/R_2 = 36$ are used instead of $1/R = 25$ as in conventional droop. The detailed of the parameter selection is discussed in Section 5.3.

4. Wind turbine system and microgrid

4.1. DFIG modelling

An overall description of a typical DFIG wind turbine (WT) is discussed briefly in this subsection. The rotor side of the WT generator is connected to the grid via a back-to-back AC/DC-DC/AC converter that regulates to extract the maximum power at various wind speeds. The mechanical power (P_{mec}) of DFIG based WT can be written as in (6) which is dependent on mechanical power coefficient C_p , a function of tip speed ratio λ and pitch angle control β , wind speed v_w , air density ρ , swept area A of turbine blade [43]

$$P_{mec} = \frac{1}{2} C_p(\lambda, \beta) \rho A v_w^3 \quad (6)$$

According to (6), at constant wind speed, C_p defines the power extraction of wind turbine. An optimum tip speed ratio at constant pitch angle is possible to achieve by adjusting the rotor speed for MPP tracking (MPPT). Therefore, MPPT regulates rotor speed reference that can capture the maximum output power at a given wind speed. In normal operation, DFIG is operated at MPP to maximize economic outcome. In order to compensate frequency variation by participating in primary frequency control, DFIG must be operated at a deloaded MPP curve and decreases/increases DFIG output depending on associated changes in frequency.

In the literature, various control approaches are discussed to perform deloaded operation [7–27]. Variable rotor speed is one of the preferred method to facilitate substantial stored kinetic energy in improving PFR. The rotor side converter of DFIG regulates variable output power by facilitating variable rotor speed. Hence, integrating additional controller in the rotor side converter can compensate for frequency deviation by means of energy exchange. Another strategy is the combined control of pitch angle regulation and rotor speed variation to achieve desired optimum deloaded power output of DFIG. The proposed strategy presents combined control of multi-gain droop control scheme with two different pitch control techniques.

4.2. Pitch angle controller

The pitch angle controller (PAC) adjusts the pitch angle of turbine blades to prevent over-speeding of rotor during high wind speeds. In the case of generator speed greater than the reference speed, PAC increases pitch angle to limit wind power output and reduce rotor speed. The pitch angle is typically adjusted to generate maximum power during a wind speed lower than the rated speed. Two different types of PACs are considered to implement combined control with the proposed multi-gain droop control: (i) Default P-type controller used in Matlab [44] and (ii) PI-type that is used in [45] and the block diagrams are shown in Fig. 4(a) and (b)). The PI regulated PAC is implemented by replacing the P controller section in Fig. 4(a). The pitch angle control with PI controller as shown in Fig. 4(b) comprises a pitch servo with a time constant of τ_2 as shown in [45]. The pitch dynamics is restricted to the following rate limit as in (7):

$$(d\beta/dt)_{min} \leq d\beta/dt \leq (d\beta/dt)_{max} \quad (7)$$

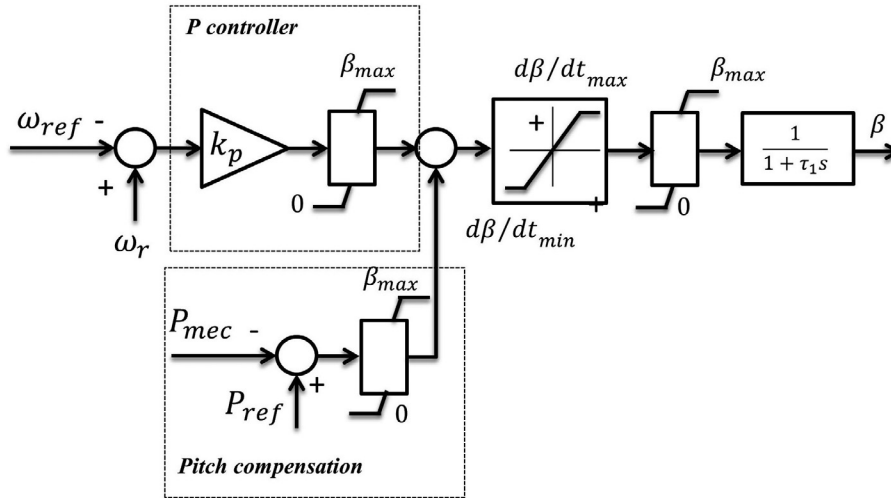
The pitch compensation controller is finally added with both controllers. The error of the actual and reference rotor speed generates an input signal to the PAC. The maximum (β_{max}) and minimum (β_{min}) pitch angle constrains the output of P and PI controller as in (8):

$$\beta_{min} \leq \beta \leq \beta_{max} \quad (8)$$

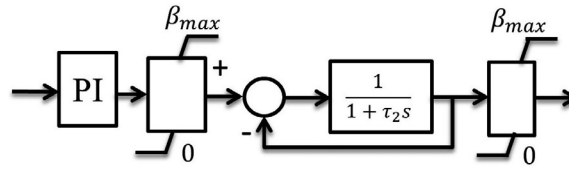
The values of pitch servo and first order filter is selected as $\tau_1 = 0.012$ [44] and $\tau_2 = 0.25$ [46] respectively.

4.3. Microgrid modeling

The proposed isolated MG is shown in Fig. 5. The power source comprises a 40 MW synchronous machine with a droop setting of 5% and an aggregated 10.5 MW wind farm. The wind farm is connected at Bus2 in the network. The connected load at Bus 2 is 25.8 MW and 4 MVar and at Bus 3 is 20.5 MW and 5MVar. The synchronous machine is equipped with Hydraulic Turbine and Governor and IEEE type 1 excitation system combined with a voltage regulator. The inertia constant (H(s)) of the synchronous machine and WTs are 3.175 s and 0.685 s, respectively. Due to limited inertial with increased wind penetration, the conventional generator may fail to provide sufficient inertial support following a contingency event. Hence, the wind turbine output power can be adjusted to regulate and improve frequency response in such a case. The reference rotor speed is 1.2 pu for the rated power out-



(a) Pitch angle control with P controller and pitch compensation



(b) Pitch angle control with PI controller

Fig. 4. The block diagram of P and PI controlled pitch angle controller.

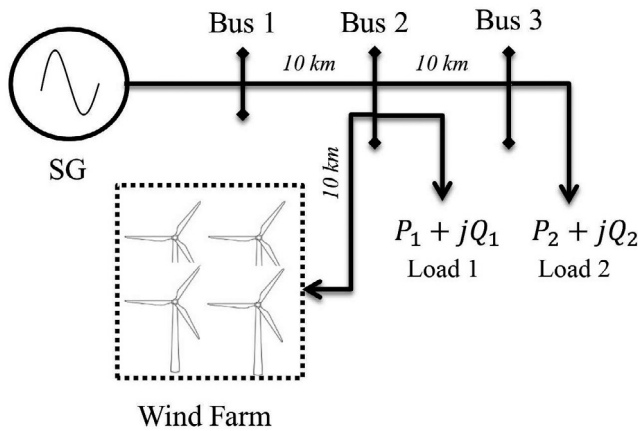


Fig. 5. Block diagram of the studied Microgrid.

put with an operating range of 0.7–1.3 pu. The wind farm is 10 km away from the load consumption center.

In order to investigate PFR performance of DFIG with the conventional and multi-gain droop control, no storage is considered in the studied isolated MG. The wind turbine is operating at 15 m/s when producing 10.5 MW power. The complete model in Simulink is shown in Fig. 6. The input signal 1 defines the maximum/minimum power output whereas signal 2 defines the median value of power output. Signals 3 and 4 represents the maximum/minimum and median frequency value, respectively. Their relationships with each other are implemented using appropriate mathematical blocks. The P/PI type Selector selects the relevant pitch angle controller depending on the input signal. The measured

frequency is taken from the grid which is compared with the nominal frequency and passed through Dead Zone droop (NOFB).

5. Simulation results and discussion

In this section, the performances of the proposed controller are discussed. The control strategies are implemented in a small isolated network using Matlab/Simulink. The simulation studies were carried out in real time using RT-LAB by OPAL-RT. For evaluation purposes, four different simulation studies are investigated and discussed in this section. In the first scenario, load event and PFR of wind farm is presented whereas the second scenario shows the variation of wind speed and PFR services by the wind farm. The third and fourth scenarios include parameter selection process for the proposed multi-gain droop and various levels of power margin of wind farm in PFR. The preferred acronym of the control strategies are conventional droop P controlled pitch (CDCP), conventional droop PI controlled pitch (CDMP), multi-gain droop P controlled pitch (SDCP) and multi-gain droop PI controlled pitch (SDMP). In this study, all the values are given in pu as apart from real values this is also widely adopted in power system studies [26–29,48,49].

5.1. Load event

A temporary step increase of 5 MW load (approximately 20%) at Bus 2 is applied for the period of 1–1.5 s. The objective is to assess the PFR response of wind farm under the proposed control approaches with the maximum wind farm power output of 0.2 pu. The overall performances are shown in Fig. 7 with and without PFR services by DFIG. The wind farm activates deloading for primary regulation when the frequency deviation differs by 100 mHz from the nominal value.

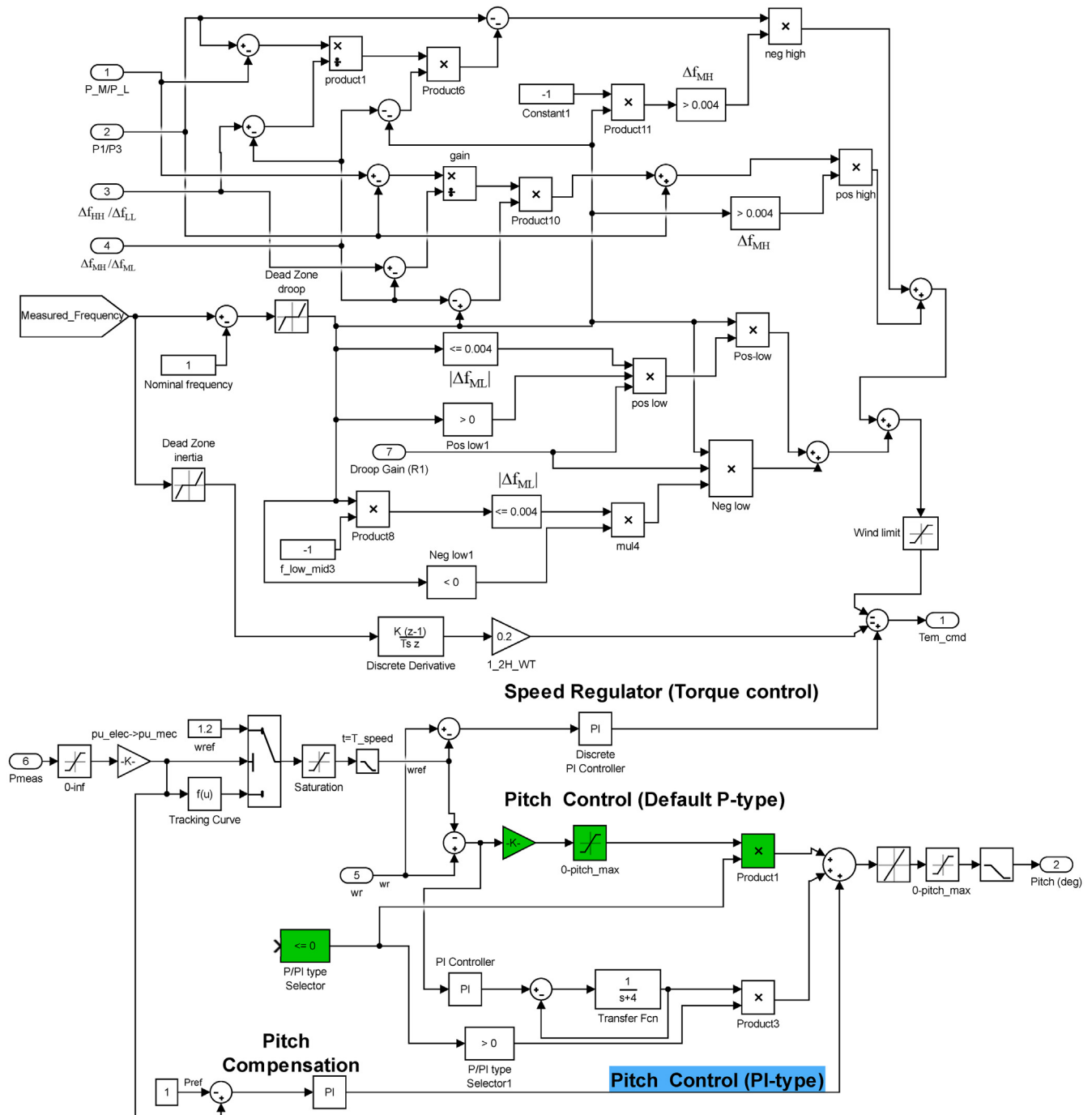


Fig. 6. The Matlab/Simulink model of multi-gain droop controlled DFIG.

The frequency response shown in Fig. 7 demonstrates that without the PFR service of wind farm, the grid experiences the highest frequency drop f_{nadir} followed by a temporary increased load event. With P controlled pitch, multi-gain droop achieves higher f_{nadir} and lower maximum frequency (f_{max}) value than the conventional droop. Moreover, multi-gain droop provides better oscillation damping than the conventional droop as the multi-gain droop reduces its contribution near the regions of lower frequency deviation. However, conventional droop possesses higher maximum frequency value and nonetheless, both droop controllers have poor oscillation damping after the clearance of disturbance event. On the contrary, with PI controlled pitch angle controller,

multi-gain droop demonstrates the best damping performance with improved f_{nadir} and lowest f_{max} value.

As expected, the output power variation of wind farm is zero when no control strategy is applied. Fig. 8 illustrates that multi-gain droop remain successful in upholding wind farm power output and executing smoother power regulation. This comparative performances can be further explained in term of rotor speed deviation of wind farm as shown in Fig. 9. At the initial stage of load event, rotor speed decreases rapidly. However, multi-gain droop holds in rotor speed variation in an optimum manner that is reflected in the smoother frequency response.

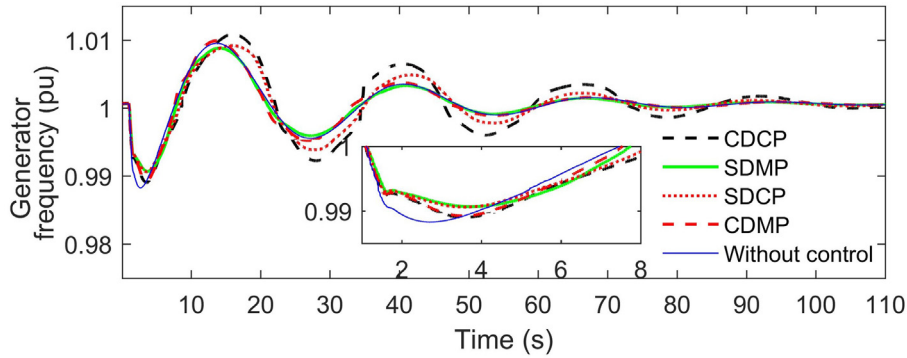


Fig. 7. The frequency of synchronous generator with load event.

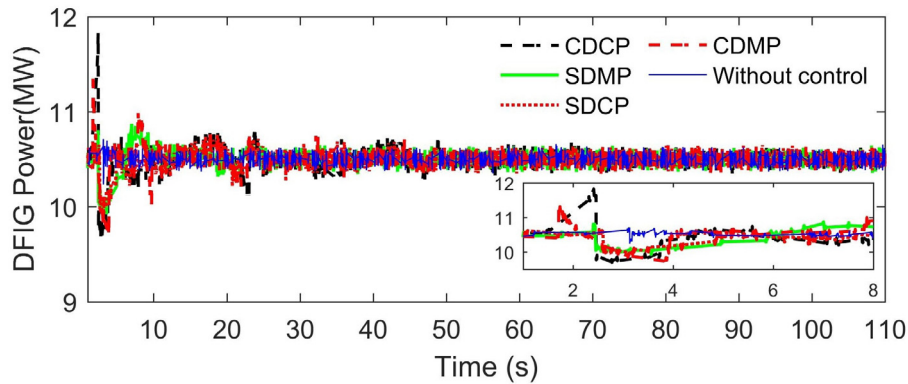


Fig. 8. DFIG power output in PFR with load event.

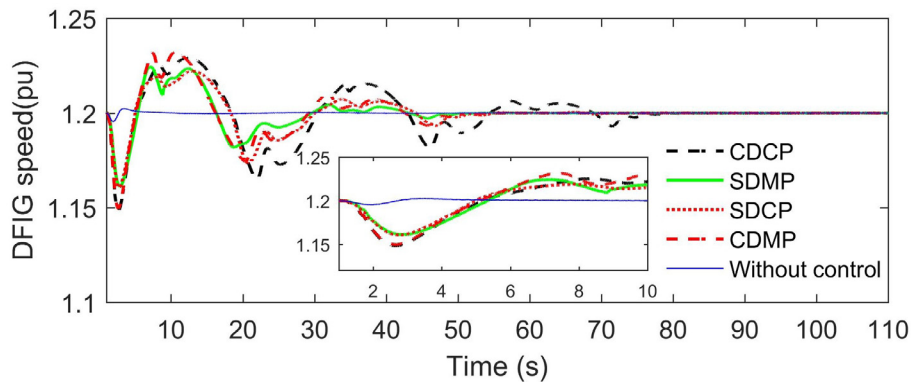


Fig. 9. Rotor speed of DFIG with load event.

The multi-gain droop with P (SDCP) and PI regulated pitch (SDMP) perform better with optimum rotor speed regulation than the conventional droop (CDCP and CDMP).

The linear relationship of P-f droop for low frequency deviations result in large variations in pitch angle as shown in Fig. 10. As it is reflected in the wind farm output power, SDMP exhibits better governance of pitch control over any other control approaches. The results illustrate that the proposed control schemes contribute more to reduce frequency drop and enhance oscillation damping with various pitch angle controllers.

The performance indice i.e the sum of squared errors of prediction (SSE) is employed for comparative performance analysis between the conventional and the proposed method. The SSE can be written as in (9):

$$SSE = \sum_{m=1}^n (x_m - y_m)^2 \quad (9)$$

where, x_m = steady state value at the initial condition and y_m = actual empirical m^{th} value.

The SSE values shown in Table 1 illustrate the comparative performance in frequency control in regard to deviation of frequency to the nominal frequency value. The table clearly suggests that the proposed multi-gain droop performs outstandingly than the conventional droop with both types of pitch angle controllers. Considering all the responses with the proposed and existing droop based control strategies, the superior performance of the proposed multi-gain droop control can be affirmed over conventional droop control.

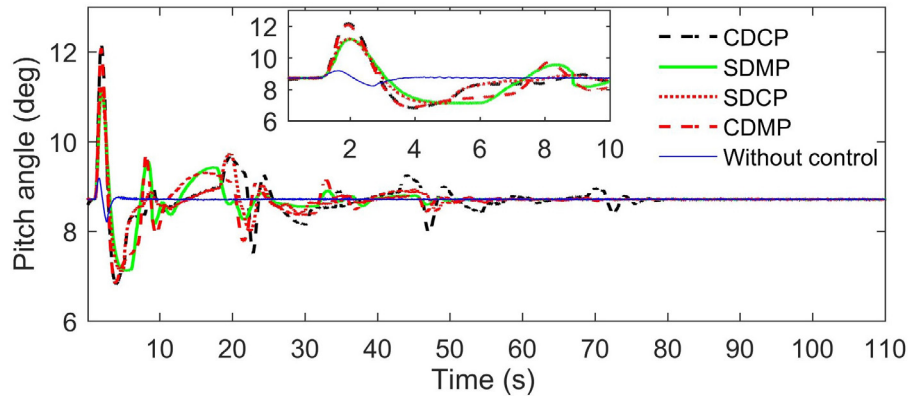


Fig. 10. Pitch angle with different controller and load event scenario.

Table 1

SSE based performance analysis of individual controllers.

| | CDCP | SDCP | CDMP | SDMP |
|------------|---------|---------|---------|---------|
| Load event | 87.2078 | 59.0311 | 51.2686 | 42.3539 |
| Wind speed | 30.4840 | 29.5387 | 18.1262 | 17.5145 |

5.2. Variation of wind speed

In order to examine the robust performance of DFIG in PFR, further time domain simulations are investigated. A temporary step decrease of wind speed from 15 m/s to 12 m/s is applied for the duration of 1–3 s and associated comparative results are illustrated in Figs. 11 and 12, respectively. Fig. 11 demonstrates that when no controller is activated, grid frequency experiences a large deviation following lower power output during the reduced wind speed. However, the same figure shows the benefits of wind farm participating in PFR regulation. The frequency deviation with the controllers is reduced by nearly half than without any control. It can be seen that the frequency nadir (f_{nadir}) is the same for all the controllers. However, it is visible that multi-gain droop performs better than the conventional droop with both pitch angle controllers, as seen previously. The multi-gain droop with the PI controlled pitch (SDMP) exhibits a faster recovery of frequency after the frequency rebound and therefore provides a smoother frequency regulation, following wind speed change.

Fig. 12 and Table 1 clearly indicates the superior outcome of the wind farm power adjustment for frequency regulation. The SDMP allows wind farm to exchange power in an optimum way than the other control approaches and achieve better frequency response. The DFIG rotor speed provides the least deviation with

the proposed SDMP control scheme. With no controllers, wind farm experiences the lowest output power drop during the reduced wind speed periods.

5.3. Parameter selection for sectional droop

In multi-gain droop control, parameter selection plays a major role in regulating and demonstrating the expected outcome. Therefore, multiple investigations were given priority before selecting the designed value for the proposed controllers. Four different cases are considered for comparative parameter selection purposes and they are based on frequency variation vs. the fixed maximum power reserve for PFR (0.2 pu). The parameters of multiple cases are outlined in Table 2 that illustrates the various levels of wind farm power adjustment with respect to the changes in frequency deviation.

Two frequency values are selected to implement and analyze the effectiveness of multi-gain droop break-point. The variable droop gain for different cases are shown in Fig. 13.

The simulation results of frequency response for the load event with different parameter selection cases are shown in Fig. 14. It can be seen that Case-3 and Case-4 demonstrates the poorest performance in the case of load change event. On the contrary, Case-2 manifests the lowest frequency nadir and the lowest maximum

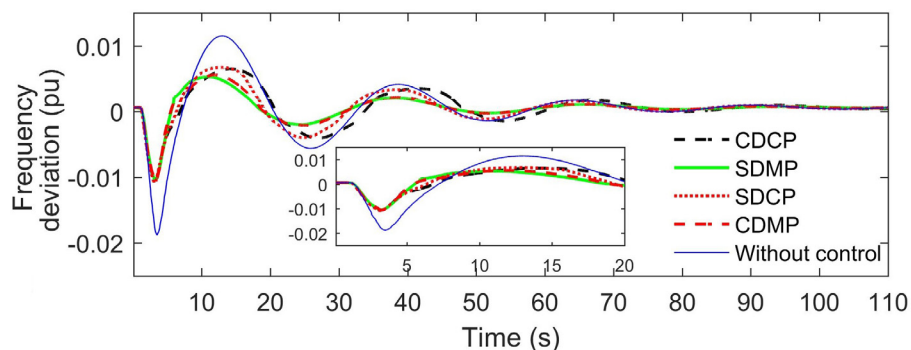


Fig. 11. The frequency of synchronous generator with wind speed variation.

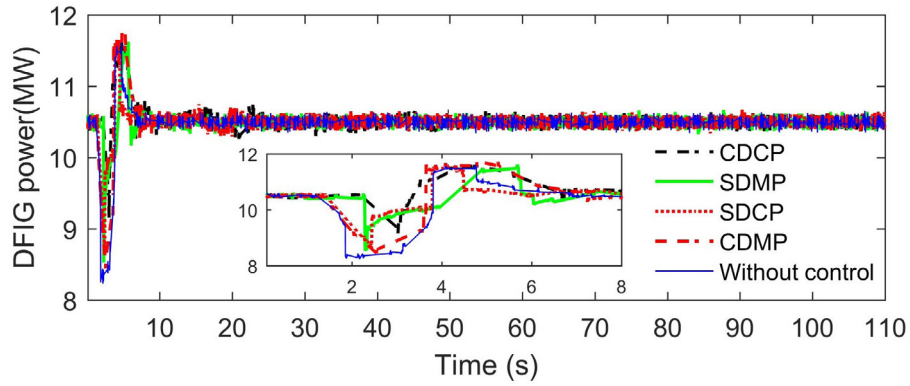


Fig. 12. DFIG power output in PFR during changes in wind speed.

Table 2
Parameter selection for multiple cases.

| | Case 1 | Case 2 | Case 3 | Case 4 |
|---------------------------------|--------|--------|--------|--------|
| $P_M = P_L$ | 0.2 | 0.2 | 0.2 | 0.2 |
| $P_1 = P_3$ | 0.074 | 0.056 | 0.037 | 0.028 |
| $\Delta f_{MH} = \Delta f_{ML}$ | 0.004 | 0.004 | 0.002 | 0.002 |
| $\Delta f_{HH} = \Delta f_{LL}$ | 0.008 | 0.008 | 0.008 | 0.008 |

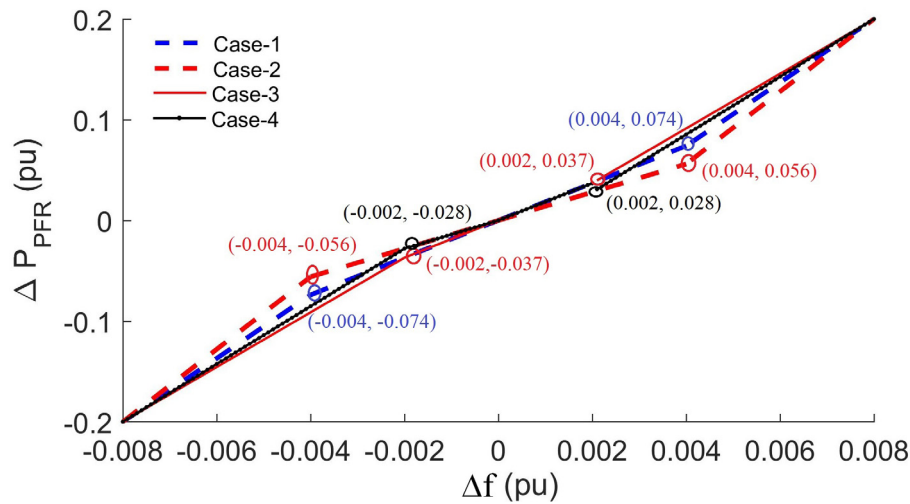


Fig. 13. The frequency of synchronous generator with wind speed variation.

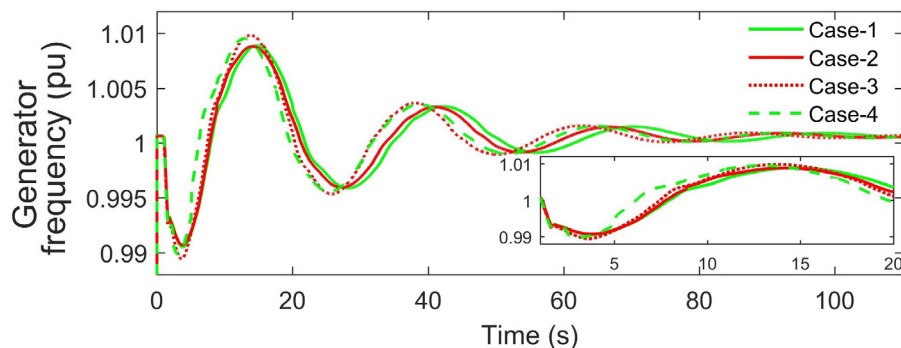


Fig. 14. The frequency of synchronous generator with load change.

frequency following the load increased scenario. In addition, Case-2 provides better oscillation damping compared to all other cases after the disturbance clearance. Similar level of superior performance is observed with Case-2 for wind speed variation. Hence, the parameters associated with Case-2 are selected for simulation purposes.

5.4. Effects of wind power participation factor in PFR

The amount of power-frequency droop in PFR defines the performance of frequency regulation. The lower droop value depicts higher participation factor of a wind farm in primary frequency regulation and the grid frequency is expected to have better oscillation damping following contingency events. On the contrary, a very high droop gain can increase wind farm output power rapidly and may result in larger oscillations or lead to instability, in extreme conditions. Hence, different levels of wind farm participation in PFR is investigated and the corresponding results are shown in Figs. 15 and 16. The selected additional participation factors are 0.1 pu and 0.3 pu with the correlated parameter of Case-2.

Fig. 15 indicates that the increased participation factor of wind farm with conventional droop (CDCP) result in large oscillations following a load change. In contrast, multi-gain droop (SDCP) demonstrates comparatively lower oscillations than CDCP. Nevertheless, SDMP provides slightly better frequency outcome and SDMP with $P_{max} = 0.2$ pu perform remarkably well in comparison to other participation factors of wind farm. The comparative performance for wind speed event is shown in Fig. 16 and it can be seen that the proposed multi-gain droop exhibits similarly superior performance. However, SDMP with 30% power margin ($P_{max} = 0.3$ pu) outperforms other participation factor. It is worth noting that when the participation factor is small (0.1 pu), multi-gain and conventional droop control provide very similar performance. However, with higher participation factor, multi-gain droop establishes its comparatively visible superior performance.

The comparative performance can be further observed through the use of SSE analysis as shown in Table 3. It can be seen that multi-gain droop has comparatively lower steady-state error than the corresponding conventional droop controller with the P and PI controlled pitch angle controllers that legitimizes its efficacy over the conventional droop control. Moreover, considering comparative steady-state error analysis shown in Table 3 further confirms the better performance for the proposed multi-gain control method, the wind power margin of 0.2 pu is selected in this paper.

5.5. Effects of higher wind power penetration in PFR

In order to validate the performance of the proposed control approach further, a higher penetration level of the wind farm is incorporated in the MG. The wind power is increased to 21 MW and the generator rated capacity is decreased to 30 MW which

causes an approximately 41% wind penetration in MG. A similar temporary load increase event in Sub-Section 5.1 is applied for the duration of $t = 1$ to 1.5 s. All the deadband limits, droop and inertia gains are the same as in Sub-Section 5.1. The simulated results of the grid frequency for various control approaches are illustrated in Fig. 17. It can be observed that with the conventional pitch, the proposed multi-gain droop control outperforms conventional droop control method in terms of frequency rise (50.55 Hz)/-drop (49.5 Hz) and damping performance during the oscillation periods. On the contrary, the frequency outcome with the proposed SDMP demonstrates the best result with a reduced drop (49.52 Hz)/rise (50.5 Hz) in frequency. The comparative results of frequency outcome for various control approaches are highlighted again in Table 4.

The pitch angle output as shown in Fig. 18 demonstrates that smoother response in pitch angle can be achieved with the proposed SDMP than any other control approaches. Furthermore, SDCP provides better regulation of pitch angle control than the conventional CDCP.

This study is carried out using RTDS which has the capability to mimic a physical system with high accuracy, a low cost solution and for this reason, RTDS is widely adopted in design and performance analysis of power system control and stability [47–49]. Compared to this study, all the previous studies [23–30] with the amalgamated droop and IE control are not implemented in real time and multi-gain is not used for droop control. Therefore, this study provides a distinct podium of integrated multi-gain control that is implemented in real-time environment in contrast to earlier studies. The conventional droop gain in the existing studies can be considered as equivalent to the CDCP/CDMP with constant droop gain. The performance analysis of the proposed SDCP/SDMP with the use of RTDS can exemplify the effectiveness of SDCP/SDMP more than the conventional approaches in earlier studies.

Based on real-time simulated results for various network conditions, several advantages can be perceived with the proposed control strategy. The minimum deviation in frequency rise/drop is realized under various contingencies with the proposed SDMP. Furthermore, SDMP damps out frequency oscillation at a faster rate and contributes to smoother pitch angle regulation than any other control methods. Moreover, the proposed control method retains the superiority over others in the case of increased wind penetration level and providing PFR. The encapsulation indicates the dominance and importance of SDMP for PFR in MG that can also be integrated into large-scale main grid.

6. Conclusion

In this research, a dynamic frequency dependent multi-gain droop control is proposed to improve frequency nadir and ensure smoother oscillation damping. The multi-gain droop is combined

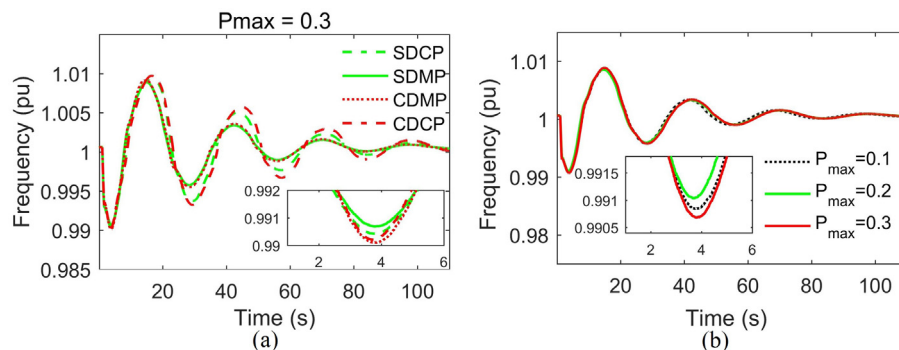


Fig. 15. The participation factor of wind farm in PFR with load change.

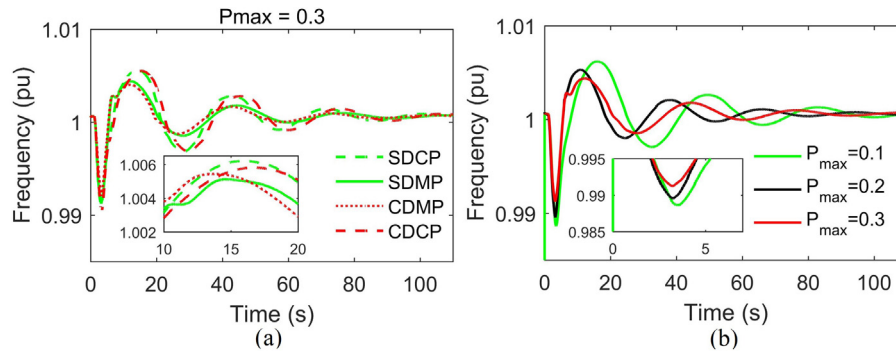


Fig. 16. The participation factor of wind farm in PFR with wind speed change.

Table 3
SSE analysis with variable wind power intensity.

| Event (P_{max}) | CDCP | SDCP | CDMP | SDMP |
|---------------------|---------|----------|---------|---------|
| Load event (0.3 pu) | 72.0402 | 64.7897 | 44.3269 | 44.3269 |
| Load event (0.2 pu) | 87.2078 | 59.0311 | 51.2686 | 40.2637 |
| Load event (0.1 pu) | 41.6907 | 35.1191 | 25.6743 | 24.6104 |
| Wind speed (0.3 pu) | 23.5068 | 22.54828 | 10.3953 | 13.3485 |
| Wind speed (0.2 pu) | 30.4840 | 29.5387 | 18.1262 | 17.5145 |
| Wind speed (0.1 pu) | 24.0403 | 25.7509 | 18.1534 | 17.6235 |

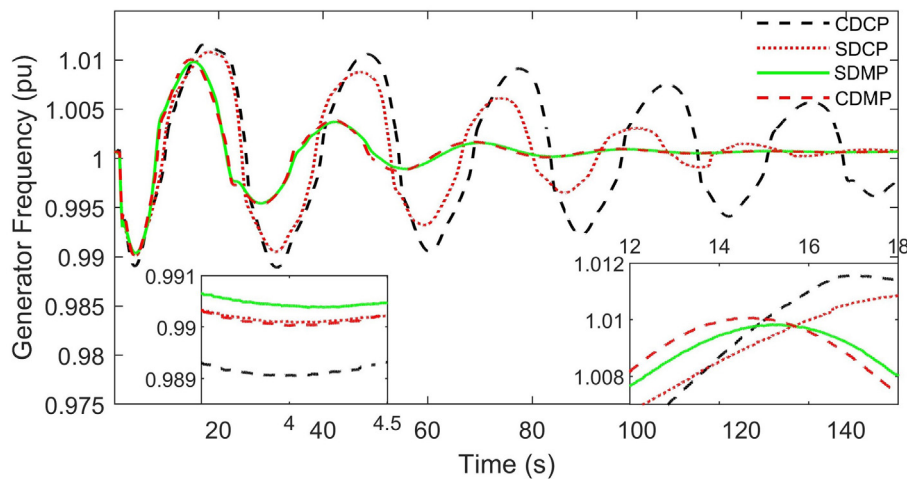


Fig. 17. The frequency of generator with higher wind penetration an load event.

Table 4
Frequency drop and rise for various control approaches.

| f(Hz) | CDCP | SDCP | CDMP | SDMP |
|------------|--------|-------|--------|-------|
| f_{drop} | 49.455 | 49.5 | 49.505 | 49.52 |
| f_{rise} | 50.6 | 50.55 | 50.505 | 50.5 |

with inertia control. In the multi-gain droop control, droop actions are divided into high and low sensitive regions, in terms of frequency deviation ranges with 20% power margin of wind farm power from the optimum position for PFR service. The proposed control scheme is coordinated with two different pitch angle controller – P and PI regulated, for comparative performance analysis purposes. In addition, a thorough investigation is carried out on selecting the most appropriate multi-gain droop parameters with various levels of wind power participation factor in frequency regulation. The simulation results indicate that the proposed multi-gain droop control scheme provides higher frequency nadir and

better frequency regulation compared to conventional droop control method with both types of pitch angle controllers. Moreover, the proposed multi-gain droop control ensures improved oscillation damping for various levels of wind farm participation in frequency regulation. Also, based on SSE analysis, 20% power margin of wind farm is perceived to be efficient for frequency regulation considering the studied contingency events. Moreover, Case2 with 28% median value is found to be the most suitable value for the multi-gain droop control parameter. In conclusion, the proposed multi-gain droop solution is realized to achieve a better outcome in terms of enhanced frequency support and optimum

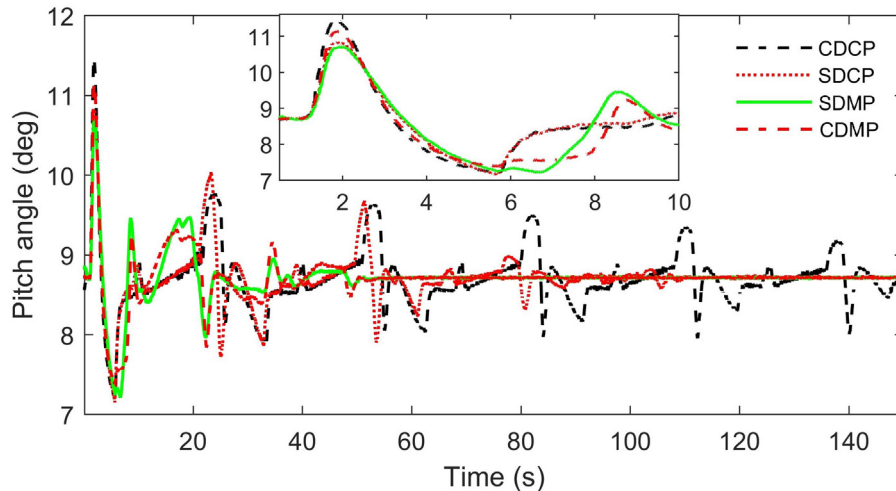


Fig. 18. The frequency of generator with higher wind penetration an load event.

frequency responses under different contingencies compared to the conventional droop control method.

Declaration of Competing Interest

The authors declare that they have no known competing financial interests or personal relationships that could have appeared to influence the work reported in this paper.

Acknowledgment

The authors would like to thank OPAL-RT for the real time simulator OP5600 and associated trainings and financial support provided by the Victoria University Research Training Program.

References

- [1] GWEC, Global Wind Report 2017. Available Online:<http://gwec.net/publications/global-wind-report-2/> (accessed 25.10.2018)..
- [2] Y. Li, S.S. Choi, C. Yang, F. Wei, Design of variable-speed dish-stirling solar-thermal power plant for maximum energy harness, *IEEE Trans Energy Convers* 301 (2015) 394–403.
- [3] G. Rashid, M.H. Ali, Fault ride through capability improvement of dfig based wind farm by fuzzy logic controlled parallel resonance fault current limiter, *Electr Power Syst Res* 146 (2017) 1–8.
- [4] U. Datta, A. Kalam, J. Shi, Battery energy storage system control for mitigating pv penetration impact on primary frequency control and state-of-charge recovery, *IEEE Trans Sustain Energy* (2019), <https://doi.org/10.1109/TSTE.2019.2904722>, pp. 1–1.
- [5] K. Idjdarene, D. Rekioua, T. Rekioua, A. Tounzi, Wind energy conversion system associated to a flywheel energy storage system, *Analog Integr Circuits Signal Process* 691 (2011) 67–73, <https://doi.org/10.1007/s10470-011-9629-2>.
- [6] X. Zeng, T. Liu, S. Wang, Y. Dong, Z. Chen, Comprehensive coordinated control strategy of pmsg-based wind turbine for providing frequency regulation services, *IEEE Access* 7 (2019) 63944–63953, <https://doi.org/10.1109/ACCESS.2019.2915308>.
- [7] C. Wu, H. Nian, B. Pang, P. Cheng, Adaptive repetitive control of dfig-dc system considering stator frequency variation, *IEEE Trans Power Electron* 344 (2019) 3302–3312, <https://doi.org/10.1109/TPEL.2018.2854261>.
- [8] Y. Zhang, A.M. Melin, S.M. Djouadi, M.M. Olama, K. Tomsovic, Provision for guaranteed inertial response in diesel-wind systems via model reference control, *IEEE Trans Power Syst* 336 (2018) 6557–6568.
- [9] M. Garmroodi, D.J. Hill, G. Verbič, J. Ma, Impact of tie-line power on inter-area modes with increased penetration of wind power, *IEEE Trans Power Syst* 314 (2016) 3051–3059.
- [10] R. You, B. Barahona, J. Chai, N.A. Cutululis, Frequency support capability of variable speed wind turbine based on electromagnetic coupler, *Renew Energy* 74 (2015) 681–688.
- [11] M. Kheshti, L. Ding, M. Nayeripour, X. Wang, V. Terzija, Active power support of wind turbines for grid frequency events using a reliable power reference scheme, *Renew Energy* 139 (2019) 1241–1254, <https://doi.org/10.1016/j.renene.2019.03.016>.
- [12] M.H. Ravanji, M. Parniani, Modified virtual inertial controller for prudential participation of dfig-based wind turbines in power system frequency regulation, *IET Renew Power Gener* 131 (2019) 155–164, <https://doi.org/10.1049/iet-rpg.2018.5397>.
- [13] V. Gevorgian, Y. Zhang, E. Ela, Investigating the impacts of wind generation participation in interconnection frequency response, *IEEE Trans Sustain Energy* 63 (2015) 1004–1012.
- [14] J.Vd. Vyver, J.D.M.D. Kooning, B. Meersman, L. Vandeveld, T.L. Vandoorn, Droop control as an alternative inertial response strategy for the synthetic inertia on wind turbines, *IEEE Trans Power Syst* 312 (2016) 1129–1138.
- [15] Y. Tan, L. Meegahapola, K.M. Muttaqi, A suboptimal power-point-tracking-based primary frequency response strategy for DFIGs in hybrid remote area power supply systems, *IEEE Trans Energy Convers* 311 (2016) 93–105.
- [16] Z. Wang, W. Wu, Coordinated control method for DFIG-based wind farm to provide primary frequency regulation service, *IEEE Trans Power Syst* 333 (2018) 2644–2659.
- [17] F. Liu, Z. Liu, S. Mei, W. Wei, Y. Yao, Eso-based inertia emulation and rotor speed recovery control for DFIGs, *IEEE Trans Energy Convers* 323 (2017) 1209–1219.
- [18] S. Ghosh, S. Kamalasadani, N. Senroy, J. Enslin, Doubly fed induction generator (DFIG)-based wind farm control framework for primary frequency and inertial response application, *IEEE Trans Power Syst* 313 (2016) 1861–1871.
- [19] S. Wang, J. Hu, S. Wang, H. Tang, Y. Chi, Comparative study on primary frequency control schemes for variable-speed wind turbines, *J Eng* 201713 (2017) 1332–1337.
- [20] R.M. Kamel, Standalone micro grid power quality improvement using inertia and power reserves of the wind generation systems, *Renew Energy* 97 (2016) 572–584.
- [21] D. Ochoa, S. Martinez, Fast-frequency response provided by DFIG-wind turbines and its impact on the grid, *IEEE Trans Power Syst* 325 (2017) 4002–4011.
- [22] Y. Hu, Y. Wu, Approximation to frequency control capability of a dfig-based wind farm using a simple linear gain droop control, *IEEE Trans Ind Appl* 553 (2019) 2300–2309, <https://doi.org/10.1109/TIA.2018.2886993>.
- [23] J. Dai, Y. Tang, Q. Wang, P. Jiang, Aggregation frequency response modeling for wind power plants with primary frequency regulation service, *IEEE Access* 7 (2019) 108561–108570, <https://doi.org/10.1109/ACCESS.2019.2933141>.
- [24] X. Zhang, X. Zha, S. Yue, Y. Chen, A frequency regulation strategy for wind power based on limited over-speed de-loading curve partitioning, *IEEE Access* 6 (2018) 22938–22951, <https://doi.org/10.1109/TPWRS.2018.2825363>.
- [25] S. Wang, K. Tomsovic, A novel active power control framework for wind turbine generators to improve frequency response, *IEEE Trans Power Syst* 336 (2018) 6579–6589, <https://doi.org/10.1109/TPWRS.2018.2829748>.
- [26] S. Chaine, M. Tripathy, D. Jain, Non dominated cuckoo search algorithm optimized controllers to improve the frequency regulation characteristics of wind thermal power system, *Eng Sci Technol Int J* 203 (2017) 1092–1105, <https://doi.org/10.1016/j.jestech.2017.05.005>.
- [27] S.P. Singh, T. Prakash, V.P. Singh, Coordinated tuning of controller-parameters using symbiotic organisms search algorithm for frequency regulation of multi-area wind integrated power system, *Eng Sci Technol Int J* (2019), <https://doi.org/10.1016/j.jestech.2019.03.007>.
- [28] M. Krpan, I. Kuzle, Dynamic characteristics of virtual inertial response provision by dfig-based wind turbines, *Electr Power Syst Res* 178 (2020), <https://doi.org/10.1016/j.epsr.2019.106005>.
- [29] A. Gupta, Y.P. Verma, A. Chauhan, Contribution of frequency linked pricing control on alfc and avr power system integrated with dfig based wind farms, *Eng Sci Technol Int J* (2019), <https://doi.org/10.1016/j.jestech.2019.06.008>.

- [30] Y. Wu, W. Yang, Y. Hu, P.Q. Dzung, Frequency regulation at a wind farm using time-varying inertia and droop controls, *IEEE Trans Ind Appl* 551 (2019) 213–224, <https://doi.org/10.1109/TIA.2018.2868644>.
- [31] Y. Jin, P. Ju, C. Rehtanz, F. Wu, X. Pan, Equivalent modeling of wind energy conversion considering overall effect of pitch angle controllers in wind farm, *Appl Energy* 222 (2018) 485–496.
- [32] H. Ye, W. Pei, Z. Qi, Analytical modeling of inertial and droop responses from a wind farm for short-term frequency regulation in power systems, *IEEE Trans Power Syst* 315 (2016) 3414–3423.
- [33] V. Gholamrezaie, M.G. Dozein, H. Monsef, B. Wu, An optimal frequency control method through a dynamic load frequency control (LFC) model incorporating wind farm, *IEEE Syst J* 121 (2018) 392–401.
- [34] C. Pradhan, C.N. Bhende, A.K. Samanta, Adaptive virtual inertia-based frequency regulation in wind power systems, *Renew Energy* 115 (2018) 558–574, <https://doi.org/10.1016/j.renene.2017.08.065>.
- [35] M.F.M. Arani, Y.A.I. Mohamed, Analysis and mitigation of undesirable impacts of implementing frequency support controllers in wind power generation, *IEEE Trans Energy Convers* 311 (2016) 174–186.
- [36] M. Hwang, E. Muljadi, J. Park, P. Sørensen, Y.C. Kang, Dynamic droop-based inertial control of a doubly-fed induction generator, *IEEE Trans Sustain Energy* 73 (2016) 924–933.
- [37] M.F.M. Arani, Y.A.I. Mohamed, Dynamic droop control for wind turbines participating in primary frequency regulation in microgrids, *IEEE Trans Smart Grid* 96 (2018) 5742–5751.
- [38] J. Zhao, X. Lyu, Y. Fu, X. Hu, F. Li, Coordinated microgrid frequency regulation based on DFIG variable coefficient using virtual inertia and primary frequency control, *IEEE Trans Energy Convers* 313 (2016) 833–845.
- [39] Y. Li, Z. Xu, J. Zhang, K.P. Wong, Variable gain control scheme of dfig-based wind farm for over-frequency support, *Renew Energy* 120 (2018) 379–391.
- [40] M. Garmroodi, G. Verbič, D.J. Hill, Frequency support from wind turbine generators with a time-variable droop characteristic, *IEEE Trans Sustain Energy* 92 (2018) 676–684.
- [41] X. Zhu, M. Xia, H.D. Chiang, Coordinated sectional droop charging control for EV aggregator enhancing frequency stability of microgrid with high penetration of renewable energy sources, *Appl Energy* 210 (2018) 936–943.
- [42] V. Knap, S.K. Chaudhary, D. Stroe, M. Swierczynski, B. Craciun, R. Teodorescu, Sizing of an energy storage system for grid inertial response and primary frequency reserve, *IEEE Trans Power Syst* 315 (2016) 3447–3456, <https://doi.org/10.1109/TPWRS.2015.2503565>.
- [43] S. Heier, R. Waddington, *Grid Integration of Wind Energy Conversion Systems*, New York, NY, USA, 2006..
- [44] R. Gagnon, Wind Farm – DFIG Detailed Model. Available Online:<https://au.mathworks.com/help/physmod/sps/examples/wind-farm-dfig-detailed-model.html> (accessed 02.09.2018)..
- [45] D. Ochoa, S. Martinez, Frequency dependent strategy for mitigating wind power fluctuations of a doubly-fed induction generator wind turbine based on virtual inertia control and blade pitch angle regulation, *Renew Energy* 128 (2018) 108–124.
- [46] T.L. Van, T.H. Nguyen, D. Lee, Advanced pitch angle control based on fuzzy logic for variable-speed wind turbine systems, *IEEE Trans Energy Convers* 302 (2015) 578–587.
- [47] C. Yang, Y. Xue, X. Zhang, Y. Zhang, Y. Chen, Real-time fpga-rtds co-simulator for power systems, *IEEE Access* 6 (2018) 44917–44926, <https://doi.org/10.1109/ACCESS.2018.2862893>.
- [48] A.S. Musleh, S.M. Muyeen, A. Al-Durra, I. Kamwa, M.A.S. Masoum, S. Islam, Time-delay analysis of wide-area voltage control considering smart grid contingences in a real-time environment, *IEEE Trans Ind Inf* 143 (2018) 1242–1252, <https://doi.org/10.1109/TII.2018.2799594>.
- [49] M. Abdelkhalek Azzouz, H.E. Farag, E.F. El-Saadany, Real-time fuzzy voltage regulation for distribution networks incorporating high penetration of renewable sources, *IEEE Syst J* 113 (2017) 1702–1711, <https://doi.org/10.1109/JSYST.2014.2330606>.